J. Earth Syst. Sci. (2023)132 17
https://doi.org/10.1007/s12040-022-02035-4

Wave modulations in the Indian coastal area due to wave–tide interactions

P Sirisha, P G Remya*, K Srinivas and T M Balakrishnan Nair

Indian National Centre for Ocean Information Services (INCOIS), Ministry of Earth Sciences (MoES), Hyderabad 500 090, Telangana, India.
**Corresponding author. e-mail: remya.pg@incois.gov.in*

MS received 30 June 2022; revised 26 September 2022; accepted 26 September 2022

The present study highlights the wave–tide interactions in a tide-dominant coast Versova, along the west coast of India. Versova is a macro tidal area and is home to fisheries. Model simulations are carried out to investigate wave–tide interactions with and without incorporating water level (WL) variations in the model setup. The simulation results are compared with the observed data at Versova. Model comparison with wave observation shows that the simulated significant wave height (Hs) reproduced the observed wave heights with an accuracy of scatter index = 8% and correlation = 0.94 with the inclusion of WL variations. The incorporation of WL variations created the energy modulations in the low-frequency part of the wave spectra, raising the periodical modulations in wave height. This low-frequency wave energy modulation is absent in the without WL simulations, resulting in underestimation of energy density which causes underestimation of Hs by ∼1 m. Hence this study strongly suggests that water level variations must be incorporated into the wave model to accurately represent wave modulations which are significant during monsoon and extreme events in the tide-dominant coastal areas.

Keywords. Wave; swell; wave–tide interaction; wave spectrum; energy modulations.

1. Introduction

Numerical modelling of wind-generated ocean waves is essential as it directly affects the near-shore processes like beach erosion, deposition, sediment transport and planning shoreline management. All coastal activities, especially coastal infrastructure development, require a clear understanding of coastal wave hydrodynamics (Parvathy *et al.* 2014). Ocean surface wave energy is significantly affected by the bathymetry, currents, and water level changes in shallow water areas (Battjes and Janssen 1978; Madsen and Sorensen 1993; Large *et al.* 1995; KiRyong and Daniela 2006). Incident wave height increases during the rising tide in a dominant tide area called 'tidal push' in which incoming tide somehow eases the passage of shoreward propagating waves. The reverse happens during the outgoing tide, which opposes the passage of waves by dissipating wave energy. This kind of wave height modulation is seen globally in all tidal basins (Davidson *et al.* 2009; Kang and Kim 2015; Lewis *et al.* 2019). The present study tries to understand the wave height modulations by the tidal elevations near the coastal areas of India.

Swells dominate wave climate around the coastal areas of India during southwest (SW) and

Published online: 18 January 2023

northeast (NE) monsoon and by wind seas during the pre-monsoon (Rao and Baba 1996; Sanil Kumar *et al.* 2000; Vethamony *et al.* 2011). Rough wave climate prevails along the west coast of India during the SW monsoon due to the dominance of strong southwest winds. The magnitude of waves is predominantly high (2–4 m) during SW monsoon; hence accurate wave climate prediction is essential to manage day-to-day maritime activities near the coastal waters. High waves and high water level (WL) variations can cause a severe impact on the coastal wave climate. A few studies showed the effect of WL variations on the wave height during extreme conditions can exist for 5–6 days. The present study is unique, exploring the impact of the WL variations on waves near the Versova coast during SW monsoon. Geographically Versova is situated along the northwest coast of India in Maharashtra. Versova is home to a large fishing community and is famous for port transactions. The people living in these areas mainly depend on fishing for their livelihood. Earth System Science Organization-Indian National Centre for Ocean Information Services (ESSO-INCOIS) delivers the potential fishing zone (PFZ) advisories using the sea surface temperature and chlorophyll data. PFZ advisory delivers information about potential fishing areas, thus reducing time and effort in searching the shoals for fish (Arun Jenish and Velmurugan 2022). On the other hand, wave forecast information ensures the fishermen's safety in the sea. Thus accurate wave height prediction is essential to manage the fishing operations in the coastal areas of India (Balakrishnan Nair *et al.* 2013; Remya *et al.* 2020; Aditya *et al.* 2022).

The people living in these areas mainly depend on fishing for their livelihood. Hence accurate wave height prediction is essential to manage the fishing operations in these coastal areas.

To analyse the wave height modulations caused by the WL elevations near Versova, we have employed the new generation spectral wave (SW) model developed by DHI. MIKE 21 SW was validated for several offshore and coastal regions by Golshani *et al.* (2005) and Jose *et al.* (2007) around the globe. Some of the researchers used the SW model to understand the Indian Ocean region wave characteristics (Aboobacker *et al.* 2009, 2011a, b, 2013, 2014; Aboobacker 2010; Remya 2012; Remya *et al.* 2012; Sabique *et al.* 2012; Balakrishnan Nair *et al.* 2013; Parvathy *et al.* 2014; Sirisha *et al.* 2015, 2017, 2019). The present study addresses the numerical modelling of waves by incorporating WL variations using MIKE 21 SW.

The manuscript is organised as follows. Sections 2 and 3 provide details of observation data and salient features of results, respectively. Section 4 gives the summary of the work and conclusions of the study.

2. Data and methodology

2.1 *Observation data*

The present study utilises the measured data from Directional Wave Rider Buoy (DWRB) at Versova coastal station (figure 1) maintained by ESSO-INCOIS. Wave rider buoy measures horizontal and vertical accelerations using two accelerometers and an onboard compass. The directional displacements obtained along the two horizontal axes are converted into wave parameters using in-built software in the buoy. Wave rider buoy measures the wave periods in the range of 1.6–30 s and directions in the range of 0°–360° with a directional resolution of 1.5°. The buoy data records are collected at a frequency of 1.28 Hz for 17 min in every half an hour.

Buoy computes the spectra with the help of fast Fourier transforms (FFT) with a high-frequency cut-off at 0.58 Hz. More details related to buoy measurements are mentioned in (Sanil Kumar *et al.* 2013). Wave parameters like significant wave height (Hs), swell wave height (Hss), wind sea wave height (Hsw) and maximum wave height (Hmax) were derived from the wave spectrum. The real-time data was received by INCOIS through the Indian National Satellite System (INSAT)/ Global System for mobile communication (GSM) modes (Sirisha *et al.* 2019).

2.2 *Water level data*

The tides near Versova are semi-diurnal (two highs and two lows) with significant diurnal inequalities. The water level data for the present study was obtained from the INCOIS tide gauge deployed at Versova. The tide gauge measurements used in the study contain tide (31 tidal constituents, including all the principal tidal constituents) and nontidal components of water levels at Versova (hence it is mentioned as water level throughout the manuscript). The tide gauge network of INCOIS consists of 36 state-of-the-art RADAR tide gauges which

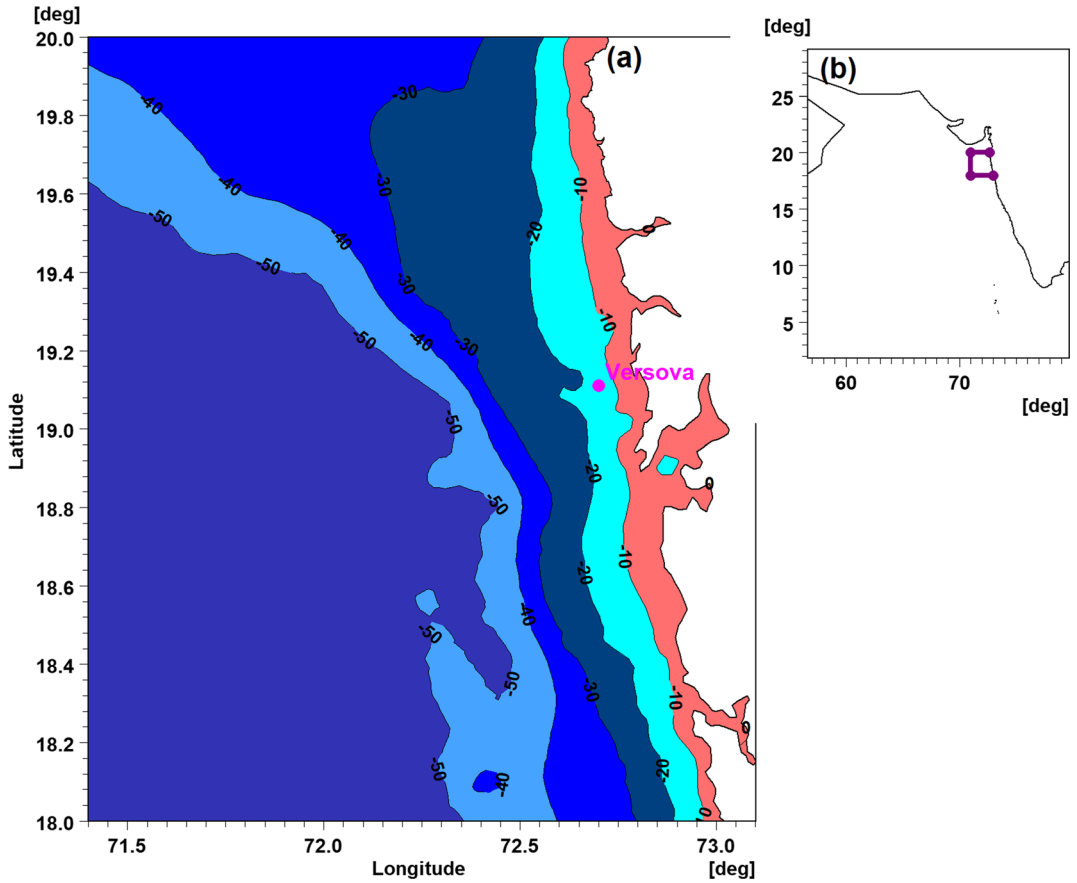

Figure 1. Plot (**a**) shows bathymetry contours and buoy location (shown with pink colour dot) and (**b**) fine resolution mesh used for the simulation of waves at Versova.

transmit near real-time data to ITEWS (Indian Tsunami Early Warning System; Unnikrishnan 2016).

2.3 *Forcing winds*

The study uses atmospheric winds generated by European Centre for Medium-Range Weather Forecasts (ECMWF) which have spatial and temporal resolutions of ∼27.5 km and 3 hours, respectively. ECMWF's database consists of atmospheric observations which are assimilated into NWP models. The output parameters obtained from these models are disseminated as medium-range forecasts that predict the weather 15 days ahead (Erik Andersson 2013). The quality of ECMWF forecast winds was ensured by Janssen *et al.* (1997) by comparing forecast winds with buoy and altimeter data. The research community extensively uses ECMF winds for the modelling and forecasting of surface waves in the Indian Ocean region (Shenoi *et al.* 2009; Balakrishnan Nair *et al.* 2013, 2014; Sirisha *et al.* 2015, 2017, 2019; Sandhya *et al.* 2018; Remya *et al.* 2020; Harikumar *et al.* 2021; Seemanth *et al.* 2021; Aditya *et al.* 2022). The present study uses the 24-hr ECMWF forecast winds for the simulation runs.

2.4 *Numerical wave model*

The study uses a state-of-the-art of third-generation spectral wind-wave model (MIKE 21 SW) developed by the Danish Hydraulic Institute (DHI), Denmark (DHI 2014). The model is based on unstructured meshes, which enhances the accuracy of wave propagation near complex areas of the coastline. The model simulates all physical characteristics of waves, i.e., wave growth, decay and transformation of waves and swells in offshore and coastal areas. The model's unique feature is the flexible mesh, i.e., fine-resolution mesh could be used in shallow regions and a coarse-resolution mesh in offshore regions. Hence this model is highly suitable for regional and local-scale wave modelling.

In MIKE 21 SW, the wave fields are represented by wave action density spectrum $N(\sigma, \theta)$ where σ and θ are relative angular frequency and direction

of wave propagation, respectively. The action density $N(\sigma, \theta)$ is related to energy density $E(\sigma, \theta)$ by,

$$N(\sigma, \theta) = \frac{E}{\sigma}. \quad (1)$$

The governing equation in MIKE 21 SW is the wave action balance equation formulated in either Cartesian or spherical coordinated. In horizontal Cartesian coordinates, the conservation equation can be written as:

$$\frac{\partial N}{\partial t} + \nabla \cdot (\overline{v} N) = \frac{S}{\sigma}, \quad (2)$$

where $N(\overline{x}, \sigma, \theta, t)$ is the action density, t is the time, $\overline{x} = (x, y)$, $\overline{v} = (c_x, c_y, c_\sigma, c_\theta)$ is the propagation velocity of a wave in the four-dimensional phase space, i.e., $\overline{x}$, σ and θ. The right-hand side of equation (2) represents the source term S which is a superposition of source functions describing various physical phenomena and is given by:

$$S = S_{\text{in}} + S_{\text{nl}} + S_{\text{ds}} + S_{\text{bot}} + S_{\text{surf}} + S_{\text{tri}}. \quad (3)$$

The physics of the model includes the phenomena like wave growth by the action of wind (S_{in}), quadruplet nonlinear wave–wave interaction (S_{nl}), dissipation due to white capping (S_{ds}), dissipation due to bottom friction (S_{bot}), dissipation due to depth-induced wave breaking (S_{surf}), and triad wave interactions (S_{tri}). The source terms of (S_{bot}), (S_{surf}) and (S_{tri}) dominate in shallow water or finite depth waters only. The incorporation of water levels significantly impacts the water depth, which further affects the relative magnitude of energy density near shallow water areas. The source functions and propagation schemes used in the SW model are described in detail and explained in Sørensen *et al.* (2004) and DHI (2014).

Bathymetry plays an essential role in wave transformations such as wave refraction, shoaling, bottom friction and depth-induced wave breaking in the nearshore modelling and hence improved bathymetry datasets of ETOPO2 (2-minute Gridded Global Relief Data) are used in the nearshore model domain (Sindhu *et al.* 2007; figure 1a). A fine-resolution mesh of (0.027°) was used in the vicinity of the Versova coast, and a mesh resolution of (0.136°) was used in the offshore waters of the domain (figure 1b). The boundary conditions are required to propagate the accurate swells in the model domain. Hence wave simulations are carried out using global multi-grid WAVEWATCH-III, and boundary parameters required for the SW model were extracted from these outputs. The quality of the WAVEWATCH-III simulated wave fields is thoroughly verified by the buoy and altimeter data by Remya *et al.* (2020) in the Indian Ocean region. MIKE 21 SW simulations were carried out from 16th June to 16th July 2016, and the results were validated with buoy data. Two separate simulations are carried out with water level (W+T) and without incorporating water level (W) during the study period.

2.5 *Methodology*

Qualitative assessment of wave parameters is carried out with the help of statistical measures such as bias, root mean square error (RMSE), scatter index (SI) and correlation coefficient (R) (Sirisha *et al.* 2017). All the statistical quantities are computed between observed and simulated wave parameters during the study period.

3. Results and discussions

The impact of water level on waves has been studied by incorporating water level variations in the nearshore simulations for one month (16th June–16th July). Figure 2 shows time series plots of observed wave parameters of significant wave height (Hs), water levels (WL), forecasted wind speed (Ws) and direction (WD). Observation shows sinusoidal variations in the wave heights ($\sim$1–3 m) at Versova during the study period. The wave heights were low (<2 m) in the initial period (16th–21st June), which then peaked due to the monsoon winds picking up, as evident from wind speed and direction (9–12 m/s and SW direction; figure 2c–d). Water level variations at the location are in the range of 1–6 m during the period. The analysis of observed Hs variations shows a low wave condition (16th–21st June) and high wave condition (22nd June–16th July) during the selected period. Hence, the following sections verify the modulation of coastal waves in the presence of water level variations in these two conditions (figure 2).

3.1 *Case 1: Impact of water level on low wave conditions (16th–21st June)*

During this period, measured Hs $<$ 1.6 m were noticed near Versova due to the prevalence of low

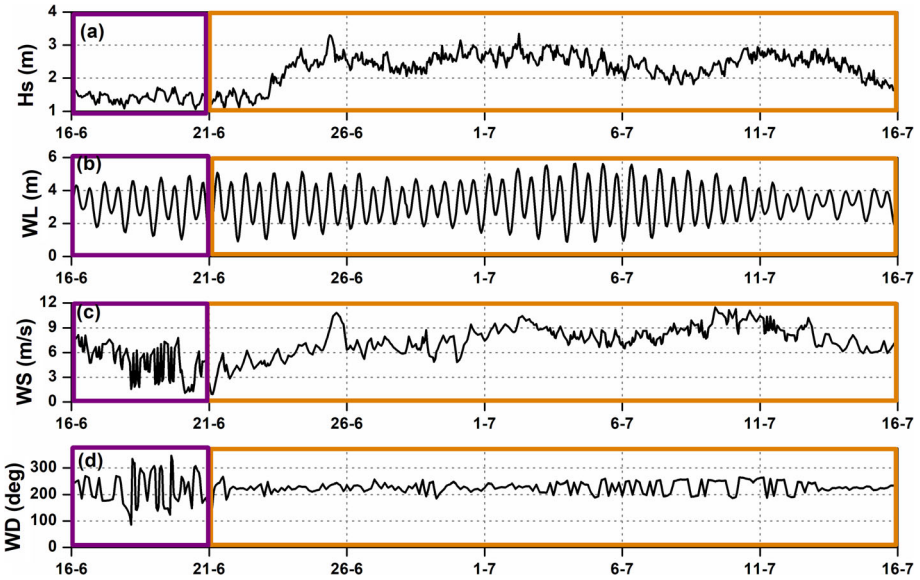

Figure 2. Observed wave parameters of (**a**) Hs (significant wave height), (**b**) WL (water level), (**c**) Ws (wind speed) and (**d**) WD (wind direction). The boxes marked with pink and orange colours refer to case 1 and 2, respectively.

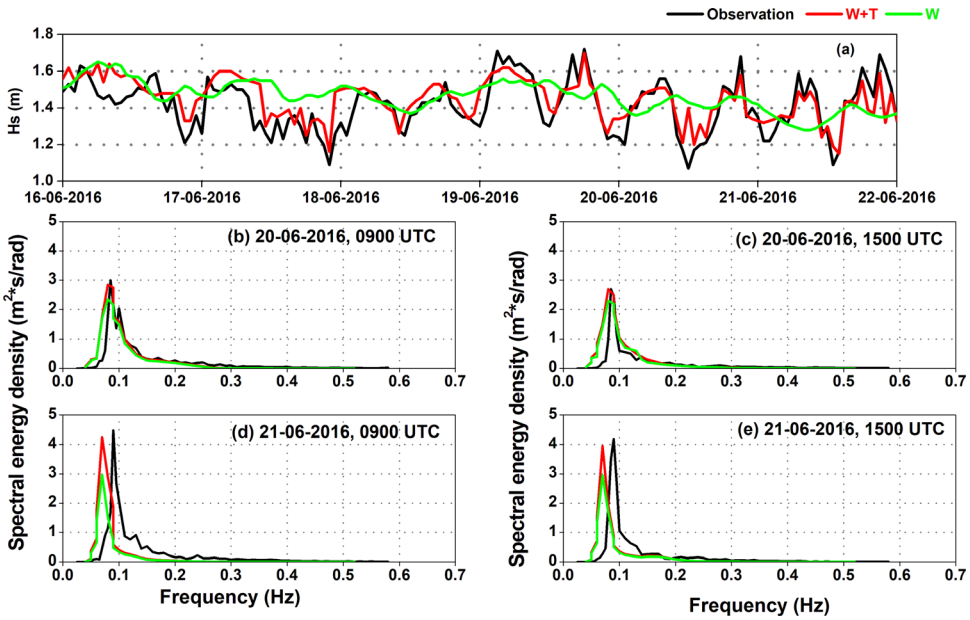

Figure 3. Plot (**a**) refers to time series plot of Hs from observation and simulations during low wave climate conditions. Plots (**b–e**) represent comparison of one dimensional spectra from observation and simulations on 20th and 21st June, 2016 at Versova.

wind (<9 m/s) conditions (figure 2a, c). The range of low and high tides varied from 1.32 to 4.69 m during this period. The simulated wave heights are compared with observed wave heights, as shown in figure 3. Wave heights from the W+T simulations closely follow the measured Hs, whereas W simulations completely missed the variations of measured Hs (figure 3a). The statistics of Hs shows low values of (bias = 0.04 m, RMSE = 0.10 m, SI = 7%) and high correlation (R = 0.77) in (W+T) compared to W (table 1). The statistics of W suggest a poor correlation (R = 0.16) between observed and simulated Hs during low wave climate.

It is noticed that water levels have varied in the range of 2–4 m during this period (figure 2b). A wave entering shallow water is affected by the physical process, such as shoaling and dissipation, due to bottom friction and wave breaking. When the water level variations are included in the simulations, the depth at each point varies, causing the same variations in the shallow water processes.

Table 1. *Model error statistics for buoy significant wave height comparison.*

	W+T				W			
	Bias (m)	RMSE (m)	SI (%)	*R*	Bias (m)	RMSE (m)	SI (%)	*R*
Case 1	0.04	0.10	7	0.77	0.05	0.16	11	0.16
Case 2	0.005	0.18	8	0.90	−0.30	0.39	17	0.76

For example, during a high tide, the wave feels less dissipation at one point due to bottom friction since the high tide adds more depth to the point, whereas in a low tide, wave energy is dissipated more at the same point due to a decrease in the water depth. This difference in energy dissipation is highly correlated with the water level variations at each location. The low-frequency part of the spectrum is mainly affected in this case as the swells have large wavelengths, and the energy modulations will be more on the low-frequency part of the spectrum (Holthuijsen 2007). When there is a low tide, water depth decreases, the low-frequency part of the spectrum experiences more dissipation, and the reverse happens during high tide. These water depth variations are absent in constant bathymetry simulations, and the energy modulations due to the nearshore process at each location will be independent of depth variations.

Energy modulations can be confirmed by comparing one-dimensional energy spectra from simulations with observations on 20th and 21st of June 2016 (figure 3b, c, d, e). Both observation and simulations show peak frequency (PF $<$ 0.125 Hz), indicating the dominance of swells near this coast. PF shift noticed on 21st June might be due to the errors in the forecast winds. The comparison of spectra shows reasonable agreement of (W+T) spectra with observation and underestimation of the low-frequency peak in W simulation. The energy dissipation is not correctly balanced in the low-frequency part of the spectrum, resulting in the underestimation of W-simulated spectra (figure 3b, c, d, e). This suggests the incorporation of water level variations in the model for accurate simulation of waves during low wind conditions.

3.2 *Case 2: Impact of water level on high wave conditions (22nd–16th July)*

This section analyses the impact of water levels on high waves (>2 m). Figure 4(a) shows the Hs comparison from 22nd June to 16th July 2016 at Versova. The range of low and high tides varied from (1.58–4.88 m) during this period. ECMWF winds of (6–12 m/s) and WL variations of (2–6 m) are noticed during the period (figure 2b, c). Hs from observations shows high waves (2–3 m) continuously throughout the period. Severe underestimation of ∼1 m is seen in the W simulation, indicating the energy dissipation is more in the absence of tide. W+T simulated Hs is mostly following the observed variance in the Hs. Error statistics of (W+T) simulation show very low values of bias (0.005 m), RMSE (0.18 m), SI (8%) and high correlation (0.90) that confirm excellent agreement of simulated Hs with observation (table 1). To understand the energy dissipation in both simulations, we have compared the one-dimensional wave spectra on 30th June and 4th July (figure 4b, c, d, e). The spectra from observation and simulations show a dominant peak on a lower frequency (PF $<$ 0.125 Hz) that confirms the predominant waves swell during these days in both simulations. The high-frequency tail of the observed spectrum (0.2–0.6 Hz) was correctly reproduced with slight underestimation in both simulations that could be attributed to the quality of forcing winds. The energy densities at the low frequencies are largely dissipated in (W) simulations. It is evident from the plots that the simulated spectra (W+T) reproduced the observation on 30th June and 4th July, but an underestimation of energy density was noticed (3–4 m^2*S/rad) in the case of W simulation. This confirms that the low-frequency wave spectra have undergone modulations incorporating water level variations.

We also analysed the influence of spring tide (2–7th July, 2016) and neap tide (12–17th July, 2016) on Hs during the study period (figure 5 and table 2). WL variations of (>5 m; figure 5a) and (2–4 m; figure 5c) are observed during the spring tide and neap tide periods near Versova, respectively. The time series comparison of wave heights during spring tide reveals that Hs from W

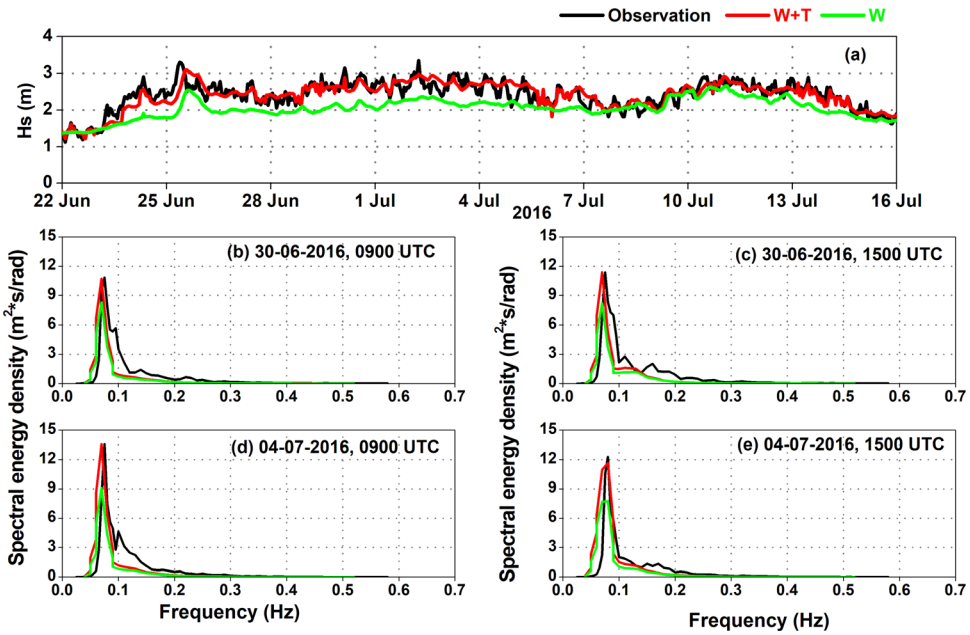

Figure 4. Plot (**a**) refers to time series plot of Hs from observation and simulations during high wave climate conditions. Plots (**b–e**) represent comparison of one dimensional spectra from observation and simulations on 30th June and 4th July, 2016 at Versova.

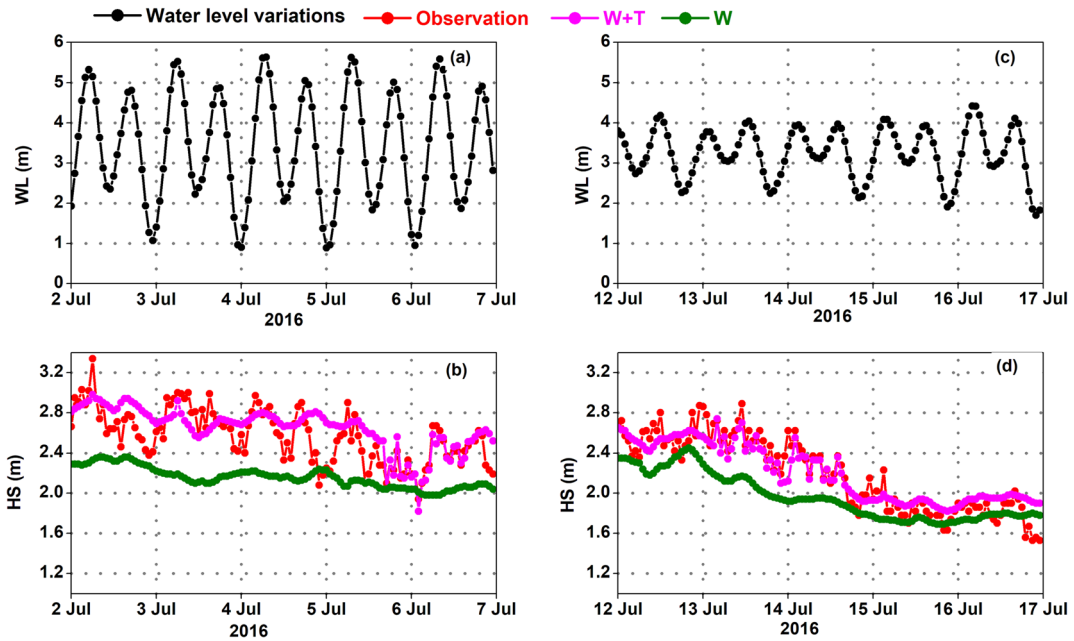

Figure 5. Time series plots of water level variations and wave heights during a spring tide (**a**, **b**) and neap tide (**c**, **d**).

Table 2. *Model error statistics for buoy significant wave height comparison during spring and neap tide periods.*

	W+T				W			
Tides	Bias (m)	RMSE (m)	SI (%)	R	Bias (m)	RMSE (m)	SI (%)	R
Spring	0.08	0.22	8	0.66	−0.41	0.48	19	0.45
Neap	0.01	0.15	7	0.93	−0.23	0.31	14	0.82

simulation could not pick the variability in the observed Hs due to the absence of WL variations (figure 5b). Wave feels less energy dissipation during spring tide since it adds more depth to the point due to very high tide. The absence of WL variations during spring tide resulted in severe underestimation of wave height by −0.41 m, high RMSE (0.48 m) and low correlation (0.45; table 2), suggesting poor agreement of Hs from W simulation during this period. During neap tide period, Hs from W simulation pick the variability in the observed Hs, with high underestimation (−0.31 m) and high RMSE (0.31 m) compared to W+T simulation (figure 5d, table 2). Wave feels high dissipation of energy due to decrease in water depth during extreme low tide.

From the above analysis, it is evident that the variations in the water level cause modulations in the wave energy and hence in the wave height. Figure 5 shows the maximum wave height (Hmax) contours from both simulations on a particular day (26th June 2016). Versova coast experiences high waves (∼5 m) in (W+T) and (∼4 m) in W simulations (figure 6). The difference in the Hmax from both simulations shows the importance of the inclusion of water level variations for accurate wave prediction in macro tidal areas.

Water level variations in (W+T) simulation modulate the water depth, which in turn modulates the wave energy and wave height parameters. The magnitude of modulations observed in wave height parameters Hs, Hmax, Hsw and Hss in (W+T) simulation are plotted in figure 7(a). Wave height modulations are observed maximum during high wave conditions compared to the low waves. The difference between the high and low wave modulations was found to be high for Hmax (9%) and Hs (5%) compared to other parameters. These modulations are changing with respect to water depth (figure 7b). The magnitude of modulations is found to be maximum (27%) near shallow water areas (∼10 m depth) and negligible (5%) in the transitional waters (∼35 m depth) off Versova. The wave starts feeling the bottom when it enters only the shallow waters, and hence the impact is more in the shallow water. The study points out that tidal variations must be incorporated into the numerical models in order to properly simulate the wave fields near tidal dominant areas. Peak period and peak direction had not shown significant difference in W+T and W simulations. Hence the present study does not address the modulations of periods and directions. However, dynamically coupled models (Atmosphere–Ocean–Tide) could be used to understand

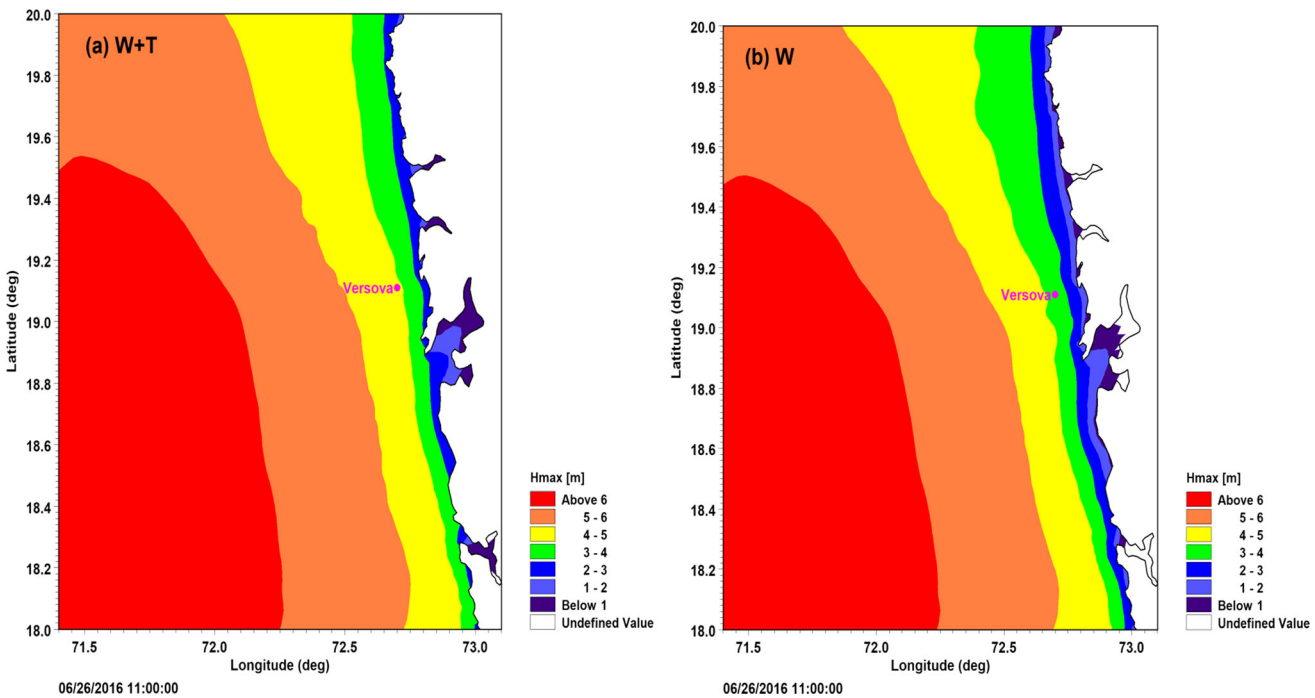

Figure 6. Contour plot of Hmax from both simulations (**a**) W+T and (**b**) W on 26th June 2016 in the study area. Refer figure 1(b) for the geographical representation of the study area.

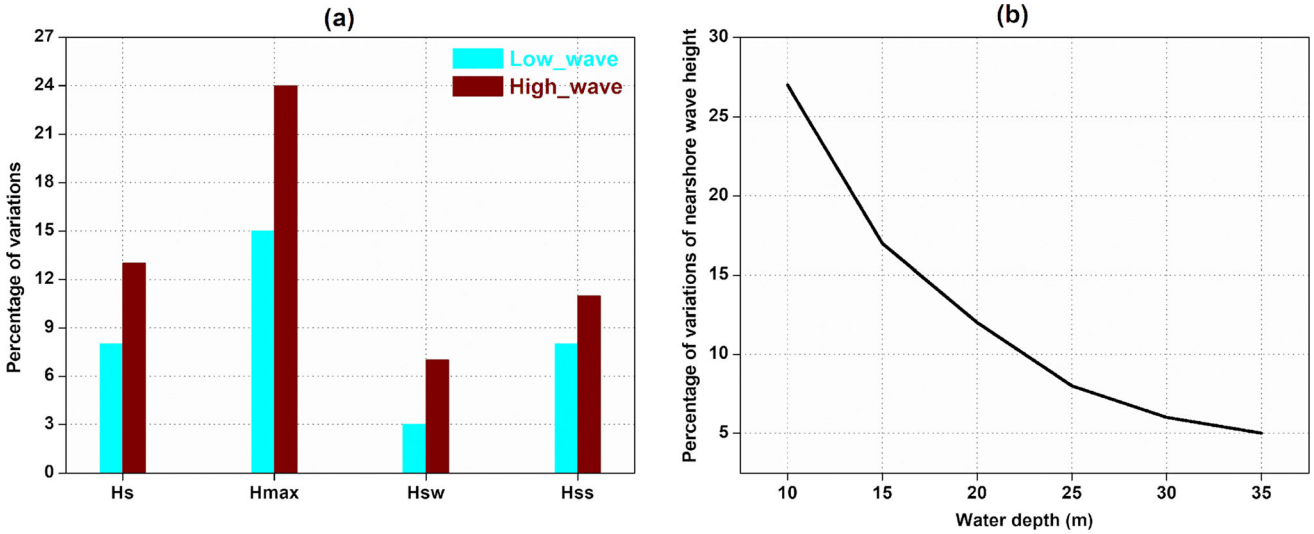

Figure 7. (**a**) Modulation of wave heights during low and high wave conditions near Versova. (**b**) Variation of nearshore wave height with respect to water depth.

the fine modulations in wave parameters near the tidal basins.

4. Conclusions

Wave–tide interactions are studied on a tide-dominant coast, Versova, along the west coast of India during the SW monsoon (June–July). MIKE 21 SW model has been used to simulate the waves near Versova during the SW monsoon. To investigate the wave–tide interactions, the wave model has been simulated with (W+T) and without (W), incorporating water level variations from a tide gauge during the SW monsoon (16th June–16th July 2016). Wave measurements at Versova showed low waves from 16th–21st June and high waves during the period (22nd June–16th July). Hence, SW model results are analysed separately under the low and high wave conditions.

During low wave conditions, comparison of simulated Hs with observation shows good agreement for W+T simulation and mismatch of high RMSE (0.10 m) and low correlation (0.16) obtained for W simulation. During high wave conditions, Hs from (W+T) simulation follows the variations as that of measured Hs, but a severe underestimation of 1 m was noticed in W simulation throughout the period (22nd June–16th July 2016). The statistics of (W+T) simulation show less bias (0.005 m), RMSE (0.18 m), SI (8%) and high correlation (0.90) that confirms excellent agreement of simulated Hs with observation. It is noticed that simulated Hs exhibited more deviation from the observation during high wave conditions.

To understand the deviation in W simulations during low wind conditions, we have compared one-dimensional energy spectra from both simulations (W+T, W) with measured spectra. Comparison of 1d spectra reveals the underestimation of energy density over the low-frequency region in the W simulation and reasonable agreement of simulated spectral energy density with measured spectra for (W+T) simulation. This confirms that low-frequency wave spectra have undergone modulations by incorporating water level variations. The interesting point noticed here is the underestimation of energy density at the low-frequency region found to be very high (3–4 m^2*S/rad) during high wind conditions in W simulation, which leads to further underestimation of Hs at Versova.

By incorporating water levels in the simulation, the wave feels less dissipation due to bottom friction during a high tide. Since high tide adds more depth to the point, wave energy is dissipated more during a low tide at the same point. This difference in energy dissipation is highly correlated with the water level variations at each location. In the present study, the low-frequency part of the spectrum is highly affected by tide modulations. The absence of water level variations in the W simulation causes the absence of energy modulation over low-frequency regions, which further results in the underestimation of energy density.

The study points out that these energy modulations are changing with respect to water depth. Near shallow water areas (10 m depth), the

magnitude of modulations is found to be maximum (27%) and negligible (5%) in the transitional waters (35 m depth) off Versova. Wave starts feeling the bottom when it enters the shallow waters, so modulations become strong only in the shallow water. The study shows that tidal variations must be incorporated into the numerical model to properly simulate the wave fields in the dominant tide areas, which significantly impacts wave forecasting. Moreover, the wave–tide interaction study is an essential topic in the scenario of sea-level rise, increasing cyclones and extreme waves along the west coast of India. A similar analysis has to be performed along with the vulnerable coastal areas of India and will be the future scope of the present work.

Acknowledgements

We thank the Director, INCOIS, and Head, ARO, for their encouragement. This research falls under OCCAS-Deep Ocean Mission, Ministry of Earth Sciences (MoES), Govt. of India. We thank MoES for the support. We also thank B Thirumal, Ajay, Arun and Dr Venkat Sheshu of INCOIS for data support. This manuscript is an ESSO-INCOIS contribution with number 474.

Author statement

Remya and Sirisha conceived the hypothesis, conceptualised the study, and designed the experiments. Material preparation and data analysis were performed by Sirisha and Remya. All authors read and approved the final manuscript.

References

Aboobacker V M 2010 Wave transformation at select locations along the Indian coast through measurements, modelling and remote sensing; Ph.D. Thesis, Goa University.

Aboobacker V M, Vethamony P, Sudheesh K and Rupali S P 2009 Spectral characteristics of the near shore waves off Paradip, India during monsoon and extreme events; *J. Nat. Hazards* **49** 311–323, https://doi.org/10.1007/s11069-008-9293-8.

Aboobacker V M, Vethamony P and Rashmi R 2011a Shamal swells in the Arabian Sea and their influence along the west coast of India; *J. Geophys. Res. Lett.* **38** 1–7, https://doi.org/10.1029/2010GL045736.

Aboobacker V M, Rashmi R, Vethamony P and Menon H B 2011b On the dominance of pre-existing swells over wind seas along the west coast of India; *J. Cont. Shelf Res.* **31** 1701–1712, https://doi.org/10.1016/j.csr.2011.07.010.

Aboobacker V M, Vethamony P, Samiksha S V, Rrashmi R and Jyoti K 2013 Wave transformation and attenuation along the west coast of India: Measurements and numerical simulations; *J. Coast. Eng.* **55(1)** 1350001-1–1350001-21, https://doi.org/10.1142/S0578563413500010.

Aboobacker V M, Seemanth M, Samiksha S V, Sudheesh K, Kerkar J and Vethamony P 2014 Sea breeze-induced wind sea growth in the central west coast of India; *J. Ocean Eng.* **84** 20–28, https://doi.org/10.1016/j.oceaneng.2014.03.030.

Aditya N D, Sandhya K G, Harikumar R and Balakrishnan Nair T M 2022 Development of small vessel advisory and forecast services system for safe navigation and operations at sea; *J. Oper. Oceanogr.* **15(1)** 52–67, https://doi.org/10.1080/1755876X.2020.1846267.

Arun Jenish and Velmurugan 2022 The role of Indian National Center for Ocean Information Services (INCOIS) in fishing industry through remote sensing; *Biotica Res. Today* **4(5)** 322–325.

Balakrishnan Nair T M, Sirisha P, Sandhya K G, Srinivas K, Sanil Kumar V, Sabique L, Arun N, Krishna Prasad B, Rakhi K and Jeyakumar C 2013 Performance of the ocean state forecast system at Indian National Centre for Ocean Information Services; C*urr. Sci.* **105** 175–181, https://www.jstor.org/stable/24092636.

Balakrishnan Nair T M, Remya P G, Harikumar R, Sandhya K G, Sirisha P, Srinivas K, Nagaraju C, Arun Nherakkol, Krishna Prasad B, Jeyakumar C, Kaviyazhahu K, Hithin N K, Rakhi Kumari, Sanil Kumar V, Ramesh Kumar M, Shenoi S S C and Shailesh Nayak 2014 Wave forecasting and monitoring during very severe cyclone Phailin in the Bay of Bengal; *Curr. Sci.* **106(8)** 1121–1125, http://drs.nio.org/drs/handle/2264/4527.

Battjes J A and Janssen J P F M 1978 Energy loss and setup due to breaking in random waves; Proc. 16th Coastal Engineering Conference, Hamburg, Germany, pp. 569–587.

Davidson Mark, Hare T and George Ken 2009 Tidal modulation of incident wave heights: Fact or fiction?; *Reef J.* **1(1)**, https://doi.org/10.2112/06-0754.1.

DHI 2014 *MIKE21 Wave modelling user guide*; DHI Water & Environment, Denmark.

Erik Andersson 2013 User guide to ECMWF forecast products; Version 1.1 New terminology, ENS initital perturbations, http://www.ecmwf.int/sites/default/files//User_Guide_V1.2_20151123.pdf.

Golshani A, Nakhaee A, Taebi S, Chegini V and Alaee M J 2005 Wave hindcast study of the Caspian Sea; *J. Mar. Eng.* **1** 19–25.

Harikumar R, Sirisha P, Anuradha Modi, Girishkumar M S, Vishnu S, Srinivas K, Rakhi Kumari, Yatin Grover, Dinesh Kumar Patro, Balakrishnan Nair T M and Mohapatra M 2021 Ocean state forecasting during VSCS Ockhi and a note on what we learnt from its characteristics: A forecasting perspective; *J. Earth Syst. Sci.* **92** 1–20, https://doi.org/10.1007/s12040-022-01850-z.

Holthuijsen L 2007 *Waves in oceanic and coastal waters*; Cambridge University Press, https://doi.org/10.1017/CB09780511618536.

Janssen P A E M, Hansen B and Bidlot J R 1997 Verification of the ECMWF wave forecasting system against Buoy and Altimeter Data; *Wea. Forecasting* **12** 763–784, https://doi.org/10.21957/1mxztz4rh.

Jose F, Kobashi F D and Stone G W 2007 Spectral wave transformation over an elongated sand shoal off South-Central Louisiana; *J. Coast Res.* **50** 757–761.

Kang K and Kim Sangil 2015 Wave–tide interactions during a strong storm event in Kyunggi Bay, Korea; *J. Ocean Eng.* **108** 10–20, https://doi.org/10.1016/j.oceaneng.2015.07.024.

KiRyong Kang and Daniela Di Iorio 2006 Depth- and current-induced effects on wave propagation into the Altamaha River estuary Georgia; *Estuar. Coast. Shelf Sci.* **66** 395–408, https://doi.org/10.1016/j.ecss.2005.09.008.

Large W G, Morzel J and Crawford G B 1995 Accounting for surface wave distortion of the marine wind profile in low-level ocean storm wind measurements; *J. Phys. Oceanogr.* **25** 2959–2971.

Lewis Matt J, Palmer Tamsin, Hashemi Resa, Robins Peter, Saulter Andrew, Brown Jenny, Lewis Huw and Neill Simson 2019 Wave-tide interaction modulates nearshore wave height; *Ocean Dyn.* **69** 367–384, https://doi.org/10.1007/s10236-018-01245-z.

Madsen P A and Sorensen O R 1993 Bound waves and triad interactions in shallow water; *J. Ocean Eng.* **20**(**4**) 359–388.

Parvathy K G, Deepthi I, Gopinath Noujas V and Thomas K V 2014 Wave transformation along Southwest coast of India using MIKE 21; *Int. J. Ocean Clim. Syst.* **5**(**1**) 23–34, https://doi.org/10.1260/1759-3131.5.1.23.

Rao C V K P and Baba M 1996 Observed wave characteristics during growth and decay: A case study; *J. Cont. Shelf Res.* **16**(**12**) 1509–1520, https://doi.org/10.1016/0278-4343(95)00084-4.

Remya P G 2012 Sea state prediction in the Indian coastal region using satellite observations and numerical model; PhD Thesis, Department of Physics, Gujarat University, http://hdl.handle.net/10603/85324.

Remya P G, Kumar R, Basu S and Sarkar A 2012 Wave hindcast experiments in the Indian Ocean using MIKE 21 SW model; *J. Earth Syst. Sci.* **21** 385–392, https://doi.org/10.1007/s12040-012-0169-7.

Remya P G, Rabi Ranjan T, Sirisha P, Harikumar R and Balakrishnan Nair T M 2020 Indian Ocean wave forecasting system for wind waves: Development and its validation; *J. Oper. Oceanogr.* **15**(**1**) 1–16, https://doi.org/10.1080/1755876X.2020.1771811.

Sabique L, Annapurnaiah K, Balakrishnan Nair T M and Srinivas K 2012 Contribution of Southern Indian Ocean swells on the wave heights in the Northern Indian Ocean: A modeling study; *J. Ocean Eng.* **43** 113–120, https://doi.org/10.1016/j.oceaneng.2011.12.024.

Sandhya K G, Murty P L N, Aditya N D, Balakrishnan Nair T M and Shenoi S S C 2018 An operational wave forecasting system for the east coast of India; *Estuar. Coast. Shelf Sci.* **202** 114–124, https://doi.org/10.1016/j.ecss.2017.12.010.

Sanil Kumar V, Ashok Kumar K and Anand N M 2000 Characteristics of waves off Goa, west coast of India; *J. Coast. Res.* **16(3)** 782–789, http://www.jstor.org/stable/4300088.

Sanil Kumar V, Dubhashi K K, Balakrishnan Nair T M and Jai Singh 2013 Wave power potential at a few shallow water locations around Indian coast; *Curr. Sci.* **104(9)** 1219–1223, https://www.jstor.org/stable/24092402.

Seemanth M, Remya P G, Suchandra Aich Bhowmick, Rashmi Sharma, Balakrishnan Nair T M, Raj Kumar and Arun Chakraborty 2021 Implementation of altimeter data assimilation on a regional wave forecasting system and its impact on wave and swell surge forecast in the Indian Ocean; *J. Ocean Eng.* **237** 1–12, https://doi.org/10.1016/j.oceaneng.2021.109585.

Shenoi Satheesh, Kumar T, Balakrishnan Nair T M, Eluri Pattabhi, Masuluri Nagaraja, Patanjali Ch, Uma Devi E, Sandhya K G and Annapurnayya K 2009 Forecasting the oceans: The oceanographic services from the Indian National Centre for Ocean Information Services; *J. Mausam (Diamond Jubilee Volume)* 225–238.

Sindhu B, Suresh I, Unnikrishnan A S, Bhatkar N V, Neetu S and Michael G S 2007 Improved bathymetric datasets for the shallow water regions in the Indian Ocean; *J. Earth Syst. Sci.* **116** 261–274, https://doi.org/10.1007/s12040-007-0025-3.

Sirisha P, Remya P G, Balakrishnan Nair T M and Venkateswara Rao B 2015 Numerical simulation and observations of very severe cyclone generated surface wave fields in the north Indian Ocean; *J. Earth Syst. Sci.* **124** 1639–1651, https://doi.org/10.1007/s12040-015-0637-y.

Sirisha P, Sandhya K G, Balakrishnan Nair T M and Venkateswara Rao B 2017 Evaluation of wave forecast in the north Indian Ocean during extreme conditions and winter monsoon; *J. Oper. Oceanogr.* **10**(**1**) 79–92, https://doi.org/10.1080/1755876X.2016.1276424.

Sirisha P, Remya P G, Anuradha Modi, Rabi Ranjan Tripathy, Balakrishnan Nair T M and Venkateswara Rao B 2019 Evaluation of the impact of high-resolution winds on the coastal waves; *J. Earth Syst. Sci.* **128** 226, https://doi.org/10.1007/s12040-019-1247-x.

Sørensen O R, Kofoed-Hansen H, Rugbjerg M and Sørensen L S 2004 A third-generation spectral wave model using an unstructured finite volume technique; *J. Coast. Eng.* (*Proceedings of the 29th Conference on Coastal Engineering*), pp. 182–186.

Unnikrishnan A S 2016 Is sea-level rising?; *J. Ocean Digest.* **3(3)** 2–4, http://drs.nio.org/drs/handle/2264/5060.

Vethamony P, Aboobacker V M, Menon H B, Ashok Kumar K and Cavaleri L 2011 Superimposition of wind season pre-existing swells off Goa coast; *J. Mar. Syst.* **87** 47–54.

Corresponding editor: C Gnanaseelan